Final Technical Report Submitted to DOE - BES (109-6062)

Nanoscale Kondo Physics and Nanomechanics of Metallic Systems from First Principles

Kohn-Sham density functional theory (DFT) is a powerful, well-established tool for the study of condensed phase electronic structure. However, there are still a number of situations where its applicability is limited. The basic theme of our research is the development of first principles electronic structure approaches for condensed matter that goes beyond what can currently be done with standard implementations of Kohn-Sham DFT. Our efforts to this end have focused on two classes of methods. The first addresses the well-known inability of DFT to handle strong, many-body electron correlation effects. Our approach is a DFT-based embedding theory, to treat localized features (e.g. impurity, adsorbate, vacancy, etc.) embedded in a periodic, metallic crystal. A description for the embedded region is provided by explicitly correlated, ab initio wave function methods. DFT, as a formally ground state theory, does not give a good description of excited states; an additional feature of our approach is the ability to obtain excitations localized in this region. We apply our method to a first-principles study of the adsorption of a single magnetic Co adatom on non-magnetic Cu(111), a known Kondo system whose behavior is governed by strong electron correlation.

The second class of methods that we are developing is an orbital-free density functional theory (OFDFT), which addresses the speed limitations of Kohn-Sham DFT. OFDFT is a powerful, $O(N)$ scaling method for electronic structure calculations.[1,2,3] Unlike Kohn-Sham DFT, OFDFT goes back to the original Hohenberg-Kohn idea of directly optimizing an energy functional which is an *explicit* functional of the density, without invoking an orbital description. This eliminates the need to manipulate orbitals, which leads to $O(N^3)$ scaling in the Kohn-Sham approach. The speed of OFDFT allows direct electronic structure calculations on large systems on the order of thousands to tens of thousands of atoms, an expensive feat within Kohn-Sham. Due to our incomplete knowledge of the exact, universal energy density functional, this speedup comes at the cost of some accuracy with respect to Kohn-Sham methods. However, OFDFT has been shown to be remarkably accurate with respect to Kohn-Sham when used in the study of nearly-free-electron-like metals, e.g., Al, for which good density functionals have been derived. Examples of past applications of OFDFT include the prediction of properties of bulk crystals, surfaces, vacancies, vacancy clusters, nanoclusters, and dislocations, as well as OFDFT-based multiscale simulations of nanoindentation in Al and Al-Mg alloys.[2,4,5,6,7,8,9]

Localized electron correlation in metals: application to the many-body Kondo state

We have been advancing a density-based embedding theory developed in our group, whose goal is to provide an accurate description of localized features embedded in periodic, metallic crystals.[10] The procedure begins with a plane-wave, Kohn-Sham DFT calculation for the total periodic system, to obtain the total density ρ_{tot}. This quantity is then partitioned as $\rho_{tot} = \rho_I + \rho_{II}$, where ρ_I and ρ_{II} are the embedded region and the background densities, respectively. The embedded region is chosen as a finite cluster containing the inhomogeneity of interest and a few surrounding atoms from the host, and should be large enough to capture the essential physics.

The problem is recast as a cluster in the presence of an effective, one-electron embedding potential υ_{emb}, whose role is to represent the periodic, metallic background. We employ a DFT model for the potential υ_{emb}, which is regarded as a functional of the total system and cluster densities, i.e.

$$\upsilon_{emb}[\rho_{tot},\rho_I] = \left(\upsilon_{Ts}[\rho_{tot}] - \upsilon_{Ts}[\rho_I]\right) + \left(\upsilon_J[\rho_{tot}] - \upsilon_J[\rho_I]\right) + \left(\upsilon_{xc}[\rho_{tot}] - \upsilon_{xc}[\rho_I]\right) + \upsilon_{ion}^{II}.$$

Here, υ_{Ts}, υ_J, and υ_{xc} denote the kinetic, Hartree, and exchange-correlation potentials, respectively, and υ_{ion}^{II} is the electron-ion potential due to the background region ions. In general, the exact form for υ_{Ts} and

υ_{xc} are not known; well-known local models (Thomas-Fermi λ-von Weizsäcker for υ_{Ts}, the local density approximation for υ_{xc}) are employed in this work. The embedded cluster problem can now be treated with the standard hierarchy of ab initio quantum chemistry methods that explicitly include electron correlation. For a given choice of ab initio theory, ρ_I and $\upsilon_{emb}[\rho_{tot},\rho_I]$ are solved self-consistently, and localized excitations are subsequently evaluated in the presence of this converged υ_{emb}.

We have made important advances in the embedding methodology, allowing for the treatment of non-trivial, realistic systems. The first is the consistent incorporation of ultrasoft pseudopotentials to represent the relatively inert core electrons in transition metals. Previous implementations of the embedding theory relied solely on norm-conserving potentials. The ultrasoft formulation significantly reduces the computational expense in the plane-wave Kohn-Sham DFT calculations;[11] however, non-standard modifications in the ultrasoft potentials were necessary to ensure consistency in the embedding. The net gain is the capability to treat transition metal systems, at a more reasonable cost in the plane-wave calculations. A second advance was made in the self-consistent search for the embedded cluster density ρ_I and embedding potential $\upsilon_{emb}[\rho_{tot},\rho_I]$. Our early work with the embedding encountered difficulties due to numerical divergences in the von Weizsäcker functional, and thus the kinetic energy contributions υ_{Ts} were frozen at some initial value. We now have a new strategy for the self-consistent search, which begins with an estimate for the background density ρ_{II}. This ρ_{II} is frozen in the embedding model, consistent with the notion that the background should be relatively inert. At each iteration of the self-consistent search, a new total density ρ_{tot}' is evaluated as $\rho_{tot}' = \rho_I' + \rho_{II}$, and the embedding potential is updated as $\upsilon_{emb} = \upsilon_{emb}[\rho_{tot}',\rho_I']$. This leads to a larger local cancellation of errors in the potential, and a more numerically stable procedure. In our current work, *all* terms in the embedding potential are allowed to update, leading to a fully self-consistent υ_{emb}.

A challenging application of the embedding methodology is the long-standing Kondo problem. The prototypical Kondo system consists of localized a magnetic impurity in a non-magnetic, metallic environment. At a material-dependent temperature T_K, an anomalous minimum in the resistivity is observed. In the Kondo picture, below T_K the conduction electrons of the host are thought to align their spins against the impurity moment, leading to an extended, open-shell singlet. The effect is thought to arise from strong many-body correlations involving the impurity moment and the conduction electrons, which is not correctly described by DFT with its approximate mean-field exchange-correlation.

Scanning tunneling microscopy (STM) experiments in 1998 reported the first direct probe of the Kondo state due to a *single* impurity moment. These experiments examined a single magnetic adatom on the (111) surface of a non-magnetic metal [Co on Au(111) and Ce on Ag(111)], and subsequent work have also explored various combinations of first-row magnetic transition metals on the (111) and (001) cuts of Cu, Ag, and Au. The STM signature ascribed to the Kondo state was found to be localized within ~10 – 60 Å of the magnetic adatom.

Up until now, our understanding of Kondo physics derives primarily from simple model Hamiltonians, i.e. the Anderson impurity model, which includes a few select interactions characterized by adjustable parameters. However, the STM experiments have opened up a whole new set of questions regarding this old problem. Given the ability to experimentally probe the Kondo state on atomic length scales, the first question that arises is: what is the detailed electronic structure of the Kondo singlet? Next, what is the nature of the low-lying excitations? How is this affected by variations in the local chemical environment? What is the role, if any, of surface states?

We have applied the embedded CI theory to examine a single Co adatom on Cu(111).[12] Correlation effects in the embedded cluster were explicitly treated using multireference single and double excitation configuration interaction (MRSDCI) theory, with the embedding theory yielding the correct singlet ground state. Note that no spin compensation is observed in a standard application of Kohn-Sham DFT, exhibiting the qualitative failure of DFT noted above. Analysis of the embedded CI ground state wave function indicates that the quenching of the Co moment is due to the formation of metal-metal bonds between Co and the neighboring Cu ions. The usual Anderson model approach does not allow for strong hybridization, i.e. bond formation, between the impurity state and conduction states, whereas our first-principles approach fully accounts for all local interactions. Thus, our work provides an alternative, chemical interpretation on the nature of the Kondo ground state.

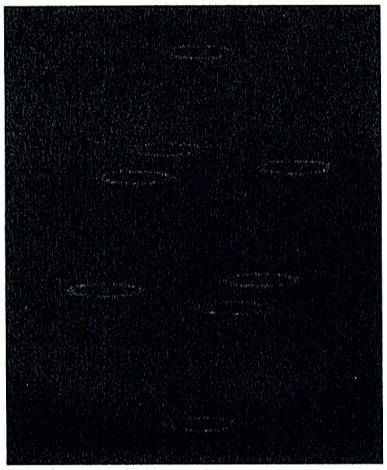

Many-body singlet ground state electron density of the embedded $CoCu_7$ cluster. Red denotes region of high density, corresponding to localized d-electrons, and blue denotes low density regions associated with metal s-electrons. Density cuts are taken along planes parallel to the Cu(111) surface, starting with the top plane passing through the Co adatom.

Future work on the Kondo problem will explore how the Co d-orbital occupations vary with changes in the local chemical environment. The lineshape of the STM Kondo resonance is due to two interfering tunneling pathways between the STM tip and 1) the localized Co d-state, and 2) the host conduction states. The experiments reveal qualitative differences in the tunneling spectra of Co on Cu(111) versus Cu(001), which was attributed to the different relative probabilities of the two pathways. In addition, an increase in the Kondo temperature T_K was seen in going from the (111) to (001) cut (from 54 K to 88 K). A first-principles estimate for the Co d-orbital populations would tell us whether it is reasonable to expect tunneling onto the Co d-levels, and a comparison of the excited states would provide insight into the scaling in T_K.

Development of new OFDFT code and application to nanowires

We have developed a second generation code to perform electronic structure calculations within the OFDFT formalism. This new code is capable of optimizing electron density, ion coordinates, and cell lattice vectors. In addition, this code is capable of finding transition state pathways using the Climbing-Image Nudged Elastic Band method.

An important new aspect of this code is the ability to handle a variety of boundary conditions. Within fully periodic boundary conditions, we have implemented the Thomas-Fermi (TF), von Weizsäcker (VW), Wang-Teter (WT) and the Wang-Govind-Carter (WGC) kinetic energy functionals.[1,2] The WGC is the most complicated, but also the most accurate OFDFT kinetic energy functional available today. Both the GGA-PBE and LDA exchange-correlation functionals are available within periodic boundary conditions.

Within free-space (aperiodic) boundary conditions, we have implemented the TF, VW, and WT kinetic energy functionals, along with the LDA exchange-correlation functional. Implementation of the WT functional presented special challenges, since the form of the response kernel is known only in reciprocal space. The WT kernel had to be decomposed into a term short-ranged in q-space, which is obtained in real-space via a Hankel transform, and a term long-ranged in q-space, which is transformed analytically.[13] Once the kernel is available in real-space, the WT energy is then obtained using a fast Fourier transform to perform a real-space convolution.

Fast algorithms to minimize the energy with respect to the electron density are critical for a useful code. We have therefore added a variety of minimization algorithms. The most useful algorithms include a nonlinear conjugate gradient algorithm, a Hessian-free truncated Newton algorithm, and a multigrid (FMG-FAS) algorithm. Previously, we have been minimizing with respect to the electron density; a major advance this year was to move to using the absolute value of the square root of the density as the relevant minimization variable, making the minimization much more stable and efficient. In addition, we are currently examining the use of other possible variables, such as the logarithm of the density.

We are now using our new OFDFT code to study properties of Al nanowires. Such wires are of interest because of their potential use in polarizing grids, biosensors, molecular electronics, and fuel cells.

Recently, Gulseren et al. [Phys. Rev. Lett. **80**, 3775 (1998)] used empirical potential molecular dynamics (EPMD) to propose exotic, noncrystalline, stable atomic structures in ultrathin Al nanowires for wire radii below a critical value, which they proposed to be on the order of a few atomic spacings. Makita et al. [J. Chem. Phys. **119,** 538 (2003)] later performed Kohn-Sham DFT calculations to examine the stability and properties of seven of the smallest of those exotic structures, and proposed that one such structure could used to create a nanoscale fuel cell. We are in the process of comparing OFDFT and KS-DFT results for the ultrathin nanowire structures examined by Makita et al. in order to verify the accuracy of OFDFT in this context. We then will move on to examine the larger exotic structures proposed by EPMD, which OFDFT can easily calculate while KS-DFT cannot, in order to develop a more complete phase diagram of aluminum nanowires as a function of wire diameter, as well as uniaxial expansion and compression.

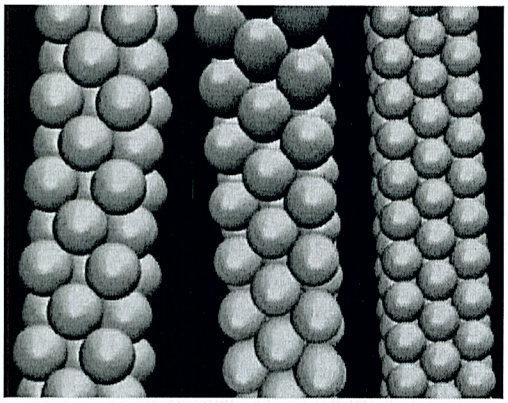

Left: [100]-oriented aluminum nanowire under 10% uniaxial tension. **Right:** Identical nanowire subject to 34% compression undergoes a phase transition to a close-packed surface structure; phase transition onset occurs at 18% compression (**middle**).

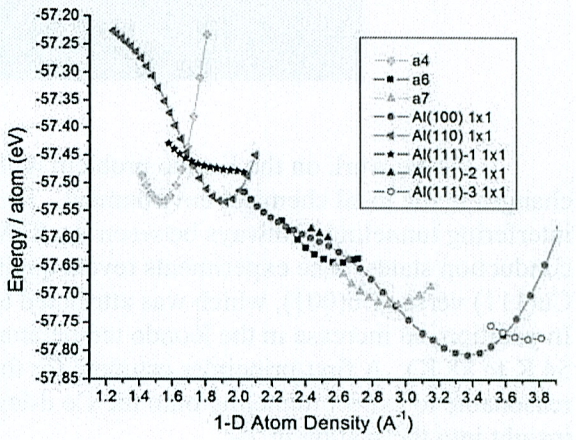

Energy per atom as a function of atomic density along the wire for various possible wire structures calculated via OFDFT. Structure labels are consistent with Gulseren et al. Phase transitions are predicted to occur as the wire is compressed and expanded.

Lastly, we are improving several aspects of the second generation code. The entire code is being parallelized, allowing for the distribution of memory to multiple nodes, so that nanosystems with more than 10,000 atoms will be accessible to study with OFDFT. Also, to reduce unwanted image effects, we would like to study nanowires with free space, or even mixed boundary conditions. This requires work in two directions: first, mixed boundary conditions must be allowed for, which presents its own set of unique challenges. Second, the more accurate but also more complex WGC kinetic energy functional must be implemented within these conditions. We also may implement local refinement within the multigrid minimizer, to improve accuracy in regions of interest.

---

[1] Y. A. Wang, N. Govind, and E. A. Carter, Phys. Rev. B **58**, 13465 (1998).
[2] Y. A. Wang, N. Govind, and E. A. Carter, Phys. Rev. B **60**, 16350 (1999).
[3] V. Lignères and E. A. Carter, in *Handbook of Materials Modeling*, S. Yip (Ed.) p.137-148, (2005); Y. A. Wang and E. A. Carter, in "Theoretical Methods in Condensed Phase Chemistry," S. D. Schwartz, Ed., within the series "Progress in Theoretical Chemistry and Physics," Kluwer, 117-84 (2000).
[4] S. C. Watson and E. A. Carter, Comp. Phys. Comm. **128**, 67 (2000).
[5] G. S. Ho, M. T. Ong, K. J. Caspersen, and E. A. Carter, to be submitted.
[6] N. Choly, G. Lu, W. E, and E. Kaxiras, Phys. Rev. B **71**, 094101 (2005).
[7] R. L. Hayes, G. S. Ho, M. Ortiz, and E. A. Carter, Phil. Mag. **86,** 2343 (2006).
[8] R. L. Hayes, M. Fago, M. Ortiz, and E. A. Carter, Multiscale Mod. Sim. **4** 359 (2005).
[9] M. Fago, R. L. Hayes, E. A. Carter, and M. Ortiz, Phys. Rev. B **70**, 100102(R) (2004).
[10] P. Huang and E. A. Carter, J. Chem. Phys. **125**, 084102 (2006).
[11] V. Cocula, C. J. Pickard, and E. A. Carter, J. Chem. Phys., **123**, 214101 (2005).
[12] P. Huang and E. A. Carter, Nano Lett. **6**, 1146 (2006), cover article.
[13] C.J. García-Cervera, Comm. Comp. Phys., submitted (2006).